The Unfolded State of NTL9 Is Compact in the Absence of Denaturant†

Burcu Anil,‡ Ying Li,‡ Jae-Hyun Cho,§ and Daniel P. Raleigh*,‡,§,||

Department of Chemistry, State University of New York, Stony Brook, New York 11794-3400, Graduate Program in Biochemistry and Structural Biology, State University of New York, Stony Brook, New York 11794, and Graduate Program in Biophysics, State University of New York, Stony Brook, New York 11794

Received March 31, 2006; Revised Manuscript Received June 8, 2006

ABSTRACT: Interest in the unfolded state of proteins has grown with the realization that this state can have considerable structure in the absence of denaturants. Natively unfolded proteins, mutations that unfold proteins under native conditions, and changes in pH that induce unfolding are attractive models for the unfolded state in the absence of denaturant. The unfolded state of the N-terminal domain of ribosomal protein L9 (NTL9) was previously shown to contain significant non-native electrostatic interactions [Cho, J. H., Sato, S., and Raleigh, D. P. (2004) *J. Mol. Biol. 338*, 827−837]. NTL9 has a mixed $\alpha-\beta$ structure and folds via a two-state mechanism. We have generated a model of the unfolded state of NTL9 in the absence of denaturant by substitution of an alanine for phenylalanine 5 located in the core of this protein. The CD spectrum of the variant, denoted as F5A, exhibits significantly less structure than the wild type; however, the mean residue ellipticity of F5A at 222 nm (−8200 deg cm^2 dmol^{-1}) is considerably larger than expected for a fully unfolded protein, indicating that residual secondary structure is populated. F5A also has more residual structure than the urea-unfolded wild type. The stability of F5A is estimated to be at least 1 kcal/mol unfavorable, showing that the unfolded state is populated to 84% or more. NMR pulsed-field gradient measurements yield a hydrodynamic radius of 16.1 Å for wild-type NTL9 and 20.8 Å for the F5A variant in native buffer. The physiologically relevant unfolded state of wild-type NTL9 is likely to be even more compact than F5A since the mutation should reduce the level of hydrophobic clustering in the unfolded state in the absence of denaturant. The hydrodynamic radius of F5A increases to 25.9 Å in 8 M urea, and a value of 23.5 Å is obtained for the wild type under similar conditions. The results show that the unfolded state of F5A in the absence of denaturant is more compact and contains more structure than the urea-unfolded form.

Analysis of the unfolded state of proteins provides important insight into protein stability and the mechanism of protein folding (*1*). Proteins can be unfolded by chaotropic agents or high temperatures. Characterization of such denatured states has often led to the impression that the unfolded proteins are random coils involving only nonspecific interactions between residues that are close in the sequence (*2*, *3*). However, the structural and thermodynamic characteristics of proteins unfolded by high temperature or denaturants may not be relevant to the unfolded state that is in equilibrium with the folded state under native conditions. It is this state which is the most relevant for folding studies. Recent developments in protein folding research have shown that unfolded states of proteins can contain significant interactions when they are investigated under mild denaturing conditions that approximately mimic the physiological environment (*4*, *5*). These interactions can be nativelike or may be of nonnative nature and disappear as folding progresses. Since the folded state is overwhelmingly populated under native conditions, it is difficult to study the physiologically unfolded state directly, except in a few cases where the unfolded state of the protein of interest is already well-populated or can be populated easily (*6*, *7*). Characterization of peptide fragments from the protein of interest, H−D exchange measurements, and pH-dependent studies are among the methods used to analyze the unfolded state indirectly (*8*−*10*). Alternatively, the folded state may be destabilized and the unfolded state populated without the use of denaturing agents. This approach can include the reduction of intramolecular disulfide bridges, removal of cofactors, mutation of residues in the hydrophobic core, or truncation of the termini of the protein (*11*−*14*).

Here, we report the characterization of a model for the unfolded state of the N-terminal domain of ribosomal protein L9 (NTL9)[1] under native conditions. NTL9 is a 56-residue globular protein with a mixed $\alpha-\beta$ topology (Figure 1). It does not require cofactors to fold, does not contain disulfide

† This work was supported by NIH Grant GM70941 to D.P.R.

* To whom correspondence should be addressed. E-mail: draleigh@notes.cc.sunysb.edu. Phone: (631) 632-9547. Fax: (631) 632-7960.

‡ Department of Chemistry.

§ Graduate Program in Biochemistry and Structural Biology.

|| Graduate Program in Biophysics.

[1] Abbreviations: ANS, 8-anilino-1-naphthalenesulfonic acid; CD, circular dichroism; $\Delta G°$, free energy of unfolding; ESI-MS, electrospray ionization mass spectrometry; HPLC, high-performance liquid chromatography; NMR, nuclear magnetic resonance; NTL9, N-terminal domain of ribosomal protein L9 from *Bacillus stearothermophilus* (residues 1−56); PFG, pulsed-field gradient; R_h, radius of hydration; TFA, trifluoroacetic acid; TMAO, trimethylamine *N*-oxide; TSP, sodium 3-trimethylsilyl-2,2,3,3-d_4-propionate.

10.1021/bi060636o CCC: $33.50
Published on Web 07/27/2006

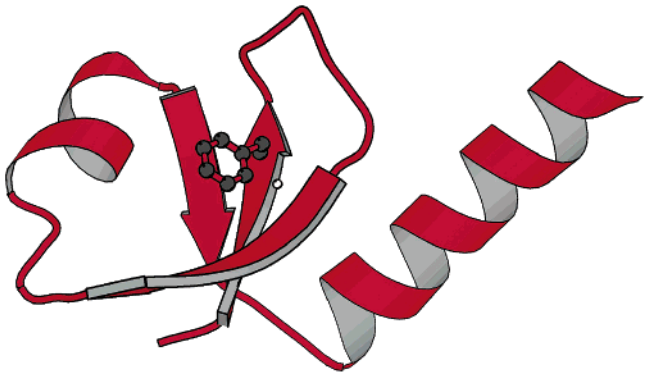

FIGURE 1: Ribbon diagram of NTL9 (PDB entry 1DIV) showing the location of F5, created using MOLSCRIPT (*32*).

bridges, and follows a two-state folding pathway (*15*, *16*). Previous studies have shown that the unfolded state of NTL9 has important non-native electrostatic interactions, the perturbation of which results in stabilization of the protein by 1.9 kcal/mol (*17*, *18*). Those studies demonstrated the presence of energetically important interactions in the unfolded state but did not provide any information about the compactness of the unfolded state or its secondary structure content. In this study, we describe the thermodynamic and structural characterization of a model for the unfolded state of the protein generated by the substitution of alanine for core residue Phe-5. The unfolded state of this mutant is estimated to be at least 84% populated under native conditions, allowing it to be studied at equilibrium. CD was used to characterize residual secondary structure, and the hydrodynamic properties of the unfolded protein were measured using NMR pulsed-field gradient (PFG) experiments (*19*). Comparison of the hydrodynamic properties of the F5A variant with those of the denaturant-induced unfolded state of the protein shows that the unfolded state is compact in the absence of denaturant.

MATERIALS AND METHODS

Protein Expression, Purification, and Characterization. The proteins were expressed as described previously (*20*) and purified by ion exchange chromatography followed by HPLC. An A−B gradient system was used for ion exchange chromatography, where buffer A consisted of 20 mM Tris-HCl and buffer B consisted of 20 mM Tris-HCl and 2 M NaCl at pH 7.5. An A−B gradient system was used for HPLC as well, where buffer A consisted of 99.9% H_2O and 0.1% TFA and buffer B consisted of 90% acetonitrile, 10% H_2O, and 0.1% TFA. The gradient that was used was from 25 to 55% B over the course of 60 min. The identities of the proteins were confirmed by electrospray ionization mass spectrometry (ESI-MS). Mass spectra calibration was performed using three standards.

Circular Dichroism Spectroscopy. CD spectra were recorded on an Aviv model 62A circular dichroism spectrometer and an Aviv model 202SF circular dichroism spectrometer equipped with Peltier temperature control systems. The experiments were carried out at 25 °C. Samples were dissolved in 20 mM sodium acetate (NaAc), 100 mM NaCl buffer at pH 5.5 and diluted to a protein concentration of 20 μM for all experiments. Protein concentrations were determined by tyrosine absorbance. Far-UV wavelength scans were performed with five repeats and a signal averaging time of 3.0 s per point, in a 1 mm cuvette, over the range of 195−260 nm. Near-UV wavelength scans were performed with five repeats and a signal averaging time of 3.0 s in a 5 mm cuvette, over the range of 260−320 nm. TMAO titrations and urea denaturation experiments were performed in a 1 cm cuvette with an averaging time of 30 s after an equilibration time of 1.5 min. Urea and TMAO concentrations were determined by measuring the refractive index.

The data from urea denaturation experiments were fit as plots of ellipticity versus denaturant concentration to the following equation (*15*):

$$f = \frac{a_n + b_n[\text{urea}] + (a_d + b_d[\text{urea}])e^{-(\Delta G^\circ_U[\text{urea}])/RT}}{1 + e^{-(\Delta G^\circ_U[\text{urea}])/RT}} \quad (1)$$

The free energy of unfolding is assumed to be a linear function of denaturant concentration:

$$\Delta G^\circ_U = \Delta G^\circ_U(H_2O) - m[\text{denaturant}] \quad (2)$$

where ΔG°_U is the apparent free energy for the N to D transition, $\Delta G^\circ_U(H_2O)$ is the free energy of unfolding in the absence of denaturant, f is the ellipticity measured from CD, T is the temperature, and R is the gas constant. a_n and b_n are used to define the ellipticity of the native state which is assumed to be a linear function of denaturant; a_d and b_d are used to define the ellipticity of the denatured state.

ANS Binding Measurements. Binding of ANS to F5A and F5A/K12M at pH 5.5 was monitored using an ISA Fluorolog spectrometer. The concentration of ANS was determined by UV absorbance, using an extinction coefficient of 8×10^3 M^{-1} cm^{-1} at 372 nm. The final concentrations were 2 μM ANS and 4 μM protein in 20 mM sodium acetate and 100 mM NaCl buffer. The samples were excited at 372 nm, and the emission spectra were recorded from 400 to 650 nm. The excitation band-pass was 2.5 nm, and the emission band-pass was 5 nm.

Sedimentation Equilibrium Measurements. The oligomeric state of F5A was determined with an experiment performed at 25 °C with a Beckman Optima XL-A analytical ultracentrifuge, using a rotor speed of 35 000 rpm. The protein was examined at concentrations of 100, 200, and 300 μM. The samples were in 20 mM sodium acetate (NaAc), 100 mM NaCl buffer at pH 5.5. Experiments were performed using 12 mm path length, six-channel, charcoal-filled, Epon cells with quartz windows. Partial specific volumes and solution density were calculated using Sednterp (*21*). The data were globally fit with a single-species model with the molecular weight treated as a fitting parameter. HID from the Analytical Ultracentrifugation Facility at the University of Connecticut was used for the fitting analysis.

NMR Measurements. One-dimensional NMR spectra of the variants were recorded on a Varian Inova 500 MHz spectrometer. All spectra were internally referenced to TSP at 0.0 ppm. The spectra were recorded at a protein concentration of 1 mM at 25 °C in 20 mM deuterated NaAc and 100 mM NaCl in 100% D_2O at pD 5.0.

Pulsed-field gradient NMR experiments were carried out on a Varian Inova 600 MHz spectrometer to measure the diffusion coefficient and the hydrodynamic radius of variants

F5A and F5V and wild-type NTL9 in no denaturant or in denaturant. Protein samples (1 mM) and 8 M urea, when it was used, were exchanged in 100% D_2O for 3 h at 25 °C and lyophilized. This process was repeated two or three times to ensure that amide protons of the proteins and all the protons of urea were fully exchanged. The pD of protein samples was adjusted to 5.5 (uncorrected) with NaOD and DCl. Urea concentrations were measured by refractometry. The sample volume was ~500 μL, and 1,4-dioxane was used as an internal standard. Susceptibility plugs were used to fix the sample height within the probe coil. The linearity of the field gradient was calibrated using a 1% (v/v) H_2O, 99% (v/v) D_2O sample and the reported diffusion coefficient (1.9×10^{-5} cm^2/s) of HOD. A modified presaturation stimulated echo pulse sequence incorporating bipolar gradient pulses was used (*22*). The diffusion delay, Δ, was 100 ms, and the gradient pulse width, δ, was 6 ms (3 ms for each component of the bipolar gradient pulse). The maximum and minimum gradient strengths were 30−45 and 5 G/cm, respectively. In all, 32 spectra were collected with an increasing gradient strength from the minimum to the maximum. A total of 128 steady-state scans were taken before every experiment started. The diffusion coefficient was independent of protein concentration over the range that was studied.

Data were processed using Felix 2000 and Sigma Plot, following standard methods (*23*), and integration of the entire aromatic region was carried out. The diffusion coefficient of dioxane was obtained by fitting the signal of the dioxane resonance versus the square of the gradient strength to a biexponential decay function, since the dioxane resonance partially overlaps with some protein resonances. The two components correspond to protein and dioxane. The reported hydrodynamic radius of 2.12 Å for dioxane was used for the calculation of R_h for both variants (*19*). Errors in the protein diffusion coefficient were estimated to be ±5% on the basis of multiple measurements and the diffusion coefficient of dioxane, so only differences of ≥10% in hydrodynamic radii were considered to be real.

RESULTS AND DISCUSSION

NTL9 F5A Is Natively Unfolded and Monomeric. Phenylalanine 5 is located on the first β-strand in the center of the hydrophobic core of NTL9 (Figure 1). Substitution with alanine at this position results in a significant difference in the far-UV CD spectrum compared to that of the wild type (Figure 2). This suggests that the deletion of the phenyl group by the alanine substitution results in significant perturbation of the packing interactions in the hydrophobic core and destabilization of the protein. The far-UV CD spectrum of F5A shows more residual structure than the urea-induced unfolded state of the wild type (Figure 2). The variant is not a molten globule since the CD signal is not close to the fully native CD intensity, which is a characteristic of molten globule states since they are rich in secondary structure (*24*). Molten globules are also characterized by their ability to bind to the hydrophobic fluorescent dye 8-anilino-1-naphthalenesulfonic acid (ANS). No significant change in the fluorescence emission of ANS can be detected upon mixing the dye with F5A, further proving that the variant is not a molten globule (Figure S1 of the Supporting Information). Smaller mutations at this site, F5L and F5V, do not affect the two-state nature of the unfolding. This provides additional

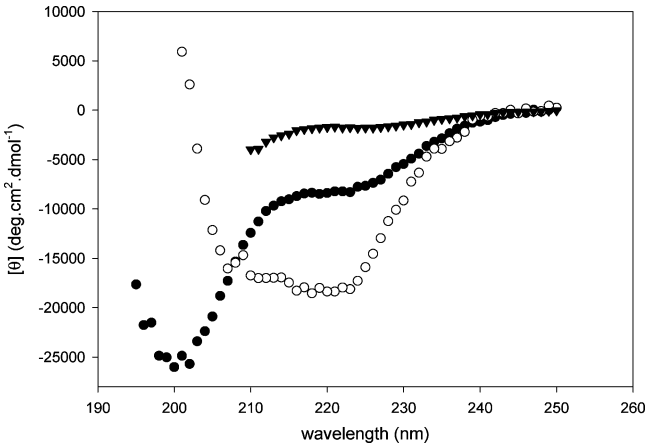

FIGURE 2: Far-UV CD spectra of NTL9 in buffered solution: (○) wild type and (●) F5A. The spectrum of the wild type in 8 M urea is also shown (▼). The spectra were recorded in 20 mM NaAC and 100 mM NaCl at pH 5.5 and 25 °C.

indirect evidence that mutations at this position do not lead to intermediate states (data not shown). The NMR spectrum of the wild type has a number of Cα protons that resonate downfield of H_2O (Figure 3A). Comparison of the one-dimensional ^{1}H spectrum of a variant and that of the wild type is a sensitive test for the integrity of the fold of the variant. The spectrum of F5A does not contain the Cα proton chemical shifts of the β-sheet in agreement with the decrease in the magnitude of the far-UV CD signal (Figure 3B).

The disruption of the hydrophobic core of the protein may result in exposure of hydrophobic residues and self-association. The oligomeric state of F5A was determined by an analytical centrifuge experiment, and the protein was found to be monomeric over the concentration range that was studied (Figure S3 of the Supporting Information). The apparent molecular mass obtained from the fit to the centrifuge data is 6202 Da, within 1% of the known actual mass (6142 Da).

F5A Populates the Unfolded State to ≥84%. It is important to know how well F5A populates the unfolded state of NTL9 and how similar F5A is to the unfolded state of the wild type. Estimation of the stability allows calculation of the relative population of the unfolded state present under native conditions. The stability of F5A could not be measured directly due to the lack of the pretransition baseline in the equilibrium denaturation experiment (data not shown). Consequently, we used an indirect approach, taking advantage of the fact that a K12M mutation has been shown to stabilize the wild-type protein (*17*). Lysine 12 is involved in non-native electrostatic interactions in the unfolded state of NTL9, and substitution with a methionine at this position results in the stabilization of the protein by almost 2 kcal/mol (*17*). If the stabilization by K12M has an additive effect on F5A, i.e., if there are no coupled interactions between Phe-5 and Lys-12, then the double mutant might be sufficiently stable to allow observation of the full equilibrium denaturation curve. In this case, the stability of F5A could be estimated by assuming that K12M has the same energetic effect on F5A as it does on the wild type.

The far-UV CD of the variant showed that the F5A/K12M double mutant has significant secondary structure (Figure S2 of the Supporting Information). The protein does not bind ANS; thus, the substitution of methionine for lysine 12 does

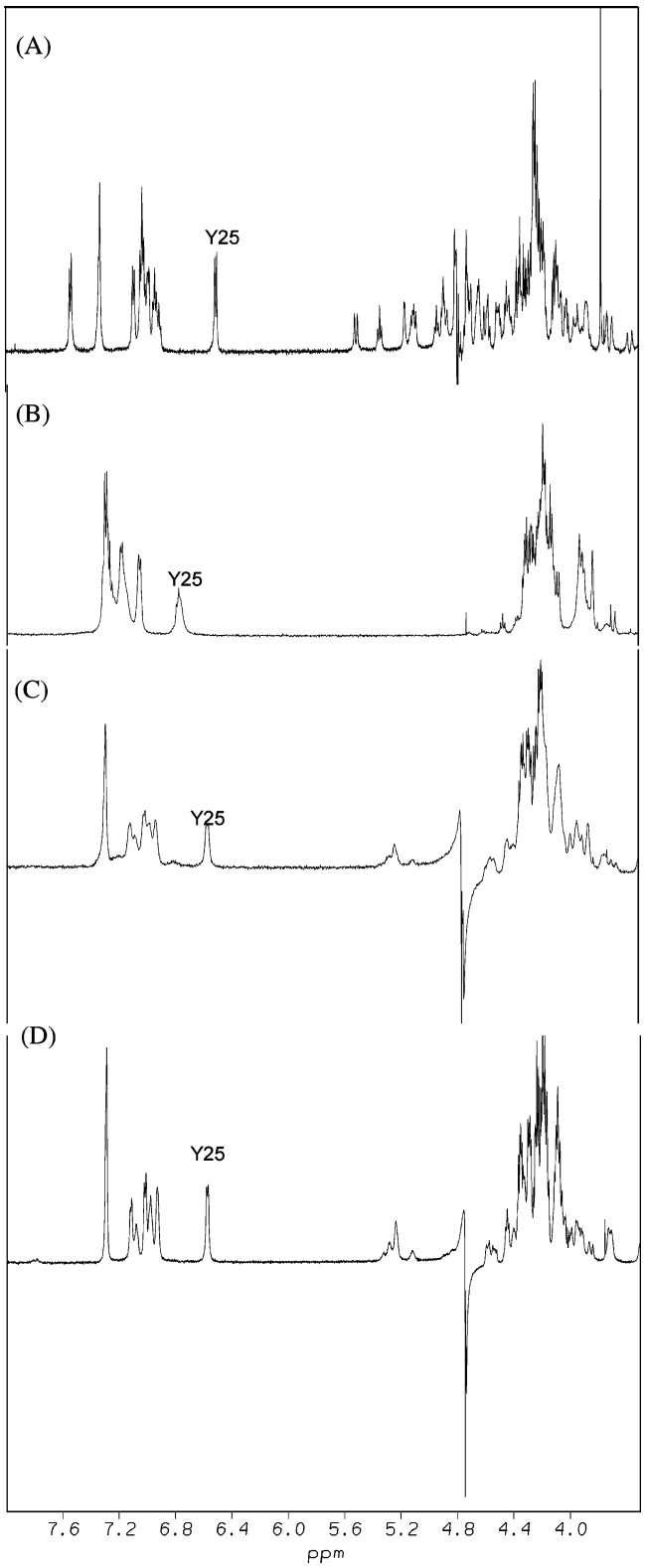

FIGURE 3: One-dimensional ^{1}H NMR spectra of NTL9: (A) wild type, (B) F5A, (C) F5A/K12M in buffer, and (D) F5A/K12M in 400 mM sulfate. The aromatic region is shown. The peak corresponding to Tyr-25 is labeled in each spectrum. All spectra were recorded in 20 mM deuterated NaAc and 100 mM NaCl in 100% D_2O at pD 5.5 (uncorrected pH-meter reading).

not induce the formation of a molten globule state for F5A (Figure S1 of the Supporting Information). The one-dimensional NMR ^{1}H spectrum of F5A/K12M reveals only one Cα proton observed in the region corresponding to the *β*-sheet (Figure 3C). Addition of the stabilizing agent sulfate

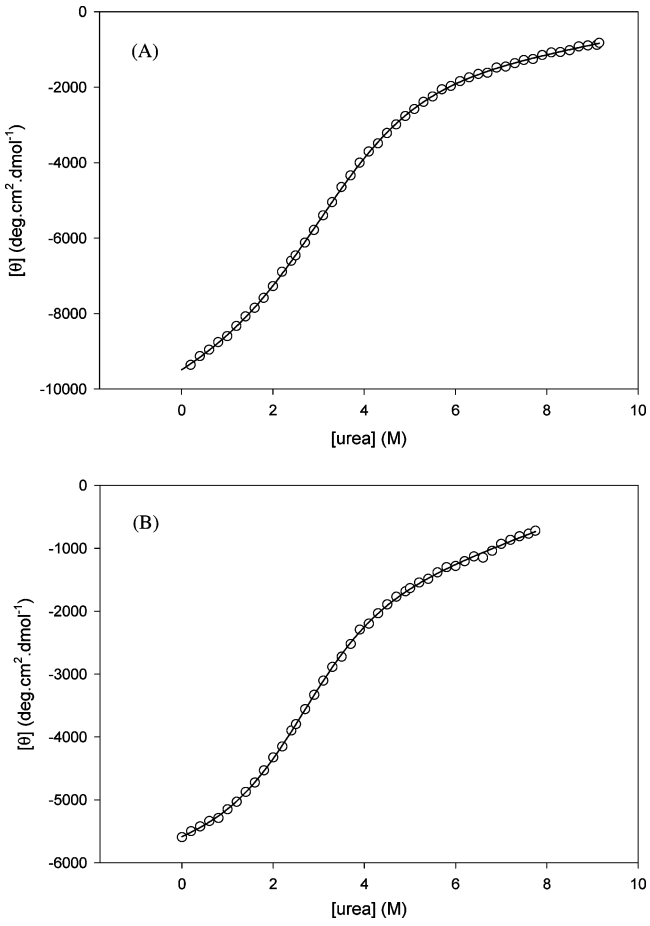

FIGURE 4: Plots of mean residue ellipticity vs urea concentration monitored in 3 M TMAO for (A) F5A/K12M and (B) F5V. The experiments were conducted at pH 5.5 in 20 mM NaAc and 100 mM NaCl at 25 °C. The lines represent the best fits to the data.

results in the appearance of more downfield-shifted Cα ^{1}H resonances, suggesting that the native state can be populated to a certain extent (Figure 3D). The urea denaturation curve of F5A/K12M does not contain a pretransition baseline (Figure S4 of the Supporting Information). There are two possibilities to explain these results. One is that the $\Delta G°$ of unfolding for F5A is so unfavorable that the additive effect of the K12M mutation is not sufficient to overcome the negative $\Delta G°$. The second possibility is that F5 and K12 have coupling interactions in the unfolded state and therefore the effect of the methionine mutation is not additive. Experiments described below argue against the second possibility.

An additional method for measuring the stability of partially folded proteins is to monitor the equilibrium unfolding in the presence of stabilizing osmolytes. Trimethylamine *N*-oxide (TMAO) is a strong osmolyte that is used to stabilize proteins (*25*). The CD signal at 222 nm of F5A/K12M was monitored by a titration experiment with TMAO. The signal intensity reached a maximum at 3.5 M TMAO. A urea equilibrium denaturation experiment was conducted in the presence of 3.0 M TMAO; the data were fit to a two-state model (Figure 4A), and the stability was calculated to be 1.78 kcal/mol (Table 1). TMAO at 3.0 M was used instead of TMAO at 3.5 M because urea is insufficiently soluble in 3.5 M TMAO to allow the full denaturation curve to be generated. These conditions are not sufficient to obtain a pretransition baseline for the equilibrium

Table 1: Equilibrium Denaturation Parameters for NTL9 and Its Variants[a]

protein	$\Delta G°$ (kcal/mol)	m (kcal mol^{-1} K^{-1})	$\Delta G°_{TMAO}$[b] (kcal/mol)	m_{TMAO}[b] (kcal mol^{-1} K^{-1})
wild type	4.30 ± 0.36	-0.66 ± 0.07	5.85 ± 0.25	−
F5A/K12M	−[c]	−	1.78 ± 0.09	-0.55 ± 0.01
F5V	−[c]	−	1.86 ± 0.07	-0.61 ± 0.01
F5V/K12M	1.99 ± 0.04	-0.63 ± 0.01	3.29 ± 0.09	-0.57 ± 0.02
K12M	6.20 ± 0.08[d]	−	7.58[e]	−

[a] All experiments were conducted in 20 mM NaAc and 100 mM NaCl at 25 °C and pH 5.5. The numbers after the ± represent the standard errors to the fit. [b] Determined in the presence of 3 M TMAO. [c] These proteins were too unstable to allow accurate direct measurement of $\Delta G°$ in H_2O. [d] Value from ref *17*. [e] Estimated on the basis of the average stabilization caused by addition of 3 M TMAO to the sample.

Scheme 1: Double Mutant Cycle for the Interactions between F5 and K12 in 3 M TMAO

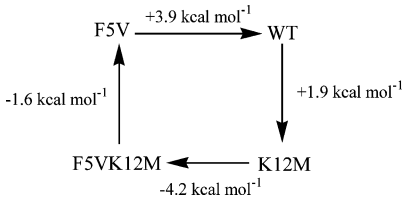

denaturation experiment of F5A; however, the stability of F5A/K12M provided an estimate of the stability of F5A under these conditions as described below.

To determine if there is any coupling between F5 and K12, we constructed a variant in which F5 was substituted with valine, denoted as F5V, and another in which the K12M mutation was introduced into F5V, denoted F5V/K12M. A valine substitution in the core still disrupts the packing interactions but is less destabilizing than an alanine. Thus, it may be possible to directly test for coupling between positions −5 and −12 by conducting a double mutant cycle analysis (*26*−*28*). The far-UV CD spectrum of F5V is similar to that of F5A, whereas the spectrum of F5V/K12M is very similar to that of the wild type (Figure S2 of the Supporting Information). The equilibrium denaturation curve of F5V does not contain a pretransition baseline; thus, the stability of both F5V and F5V/K12M was measured in 3.0 M TMAO (Figure 4B,C). The $\Delta G°$ values are 1.86 and 3.29 kcal/mol for F5V and F5V/K12M, respectively (Table 1). The m values determined for the variants in the presence of TMAO show some variations when compared to the wild-type m value. The nature of the interactions between TMAO and proteins is understood to a certain extent (*29*, *30*), and high concentrations of this osmolyte may cause differences in the surface area of the protein exposed upon denaturation. The coupling energy between two residues of interest was calculated using eq 3:

$$\Delta\Delta G°_{coupling} = \Delta G°_{WT} - \Delta G°_{F5V} - \Delta G°_{K12M} + \Delta G°_{F5V/K12M} \quad (3)$$

The thermodynamic parameters are given in Table 1, and the analysis is shown in Scheme 1. The stability of K12M could only be estimated on the basis of the average increase in the stability created by the presence of 3 M TMAO because the protein is too stable to unfold in 3 M TMAO. The estimated $\Delta G°$ value for K12M is 7.58 kcal/mol. The

Scheme 2: Double Mutant Cycle for the Interactions between F5 and K12 in Buffer

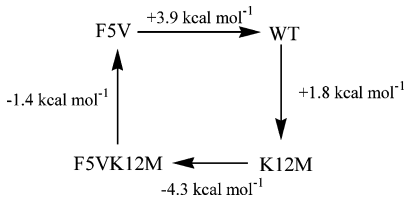

calculated coupling energy is −0.3 kcal/mol. Given that the $\Delta G°$ for K12M had to be estimated and given the error range for the individual $\Delta G°$ values, this value is not significantly different from zero, showing that there are no coupling interactions between F5 and K12. An alternative approach to calculating the coupling energy is to use the $\Delta G°$ values obtained in the absence of TMAO. Individual equilibrium denaturation experiments were carried out for F5V in the presence of 2.5 and 3.5 M TMAO. The free energy of unfolding is known to depend on TMAO concentration in a linear fashion (*25*). The linear extrapolation of the $\Delta G°$ values gives a $\Delta G°$ of 0.41 kcal/mol for F5V in H_2O. When this value is used together with the $\Delta G°$ values of the other components of the double mutant cycle analysis which are obtained in the absence of TMAO, the coupling energy is measured to be −0.32 kcal/mol (Scheme 2). Again this value is not significantly different from zero but is in agreement with the value obtained from the first analysis. We conclude that F5 and K12 do not have coupled interactions. These control experiments suggest that the effects of mutations at positions −5 and −12 should be additive and validate the approach used to estimate the stability of F5A. Thus, to a first approximation, we can assume that the lysine to methionine mutation increases the stability of the F5 variants by 1.9 kcal/mol. The stability of F5A can now be estimated if the stability of the F5A/K12M variant is known. Equilibrium denaturation experiments were conducted for this variant in 2.5 and 3.5 M TMAO, and the $\Delta G°$ value in the absence of TMAO was calculated to be 0.9 kcal/mol by linear extrapolation. When the contribution of K12M is subtracted, the free energy of unfolding of F5A is estimated to be −1.0 kcal/mol. This value corresponds to 84% population of the unfolded state.

If the folded state were populated by 16% and the interconversion between the unfolded and folded forms was slow on the NMR time scale, then we would expect to see minor peaks in the spectrum of F5A arising from folded resonances. No such peaks are visible in the aromatic region, indicating that either the population of the folded state is even lower than our estimate or the system is in fast exchange. The assumption of fast to intermediate fast exchange allows an alternative estimation of the population of the unfolded state based upon the observed chemical shift of the resolved ring proton resonances of Y25. The estimate requires values for the folded and unfolded state chemical shifts. If we use the observed value in 8 M urea as the unfolded state chemical shift and use the value measured in the presence of the stabilizing agent sulfate for the fully folded form, we obtain an estimated population of 11% for the folded state. If we use the wild-type chemical shift as our estimate for the folded state, we obtain a folded population of 7.5% for the F5A mutant. These two estimates

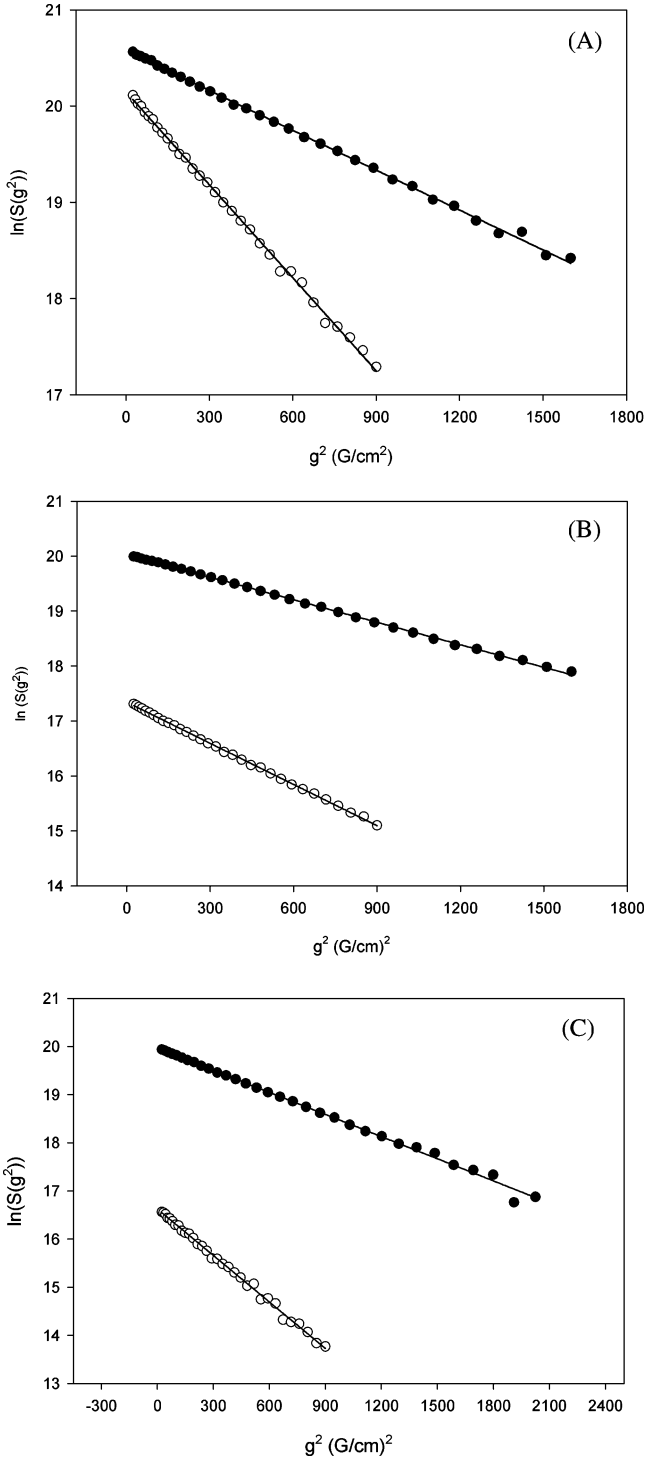

FIGURE 5: Plots of the natural logarithm of the signal intensities vs the square of the field gradient strength in the PFG diffusion experiments for NTL9: (A) wild type, (B) F5A, and (C) F5V in 100% D_2O at pD 5.5 (uncorrected pH-meter reading). White circles represent data for the sample in buffered solution, and black circles represent data for the sample in 8 M urea. The lines represent the linear regression fits, and the slopes are proportional to the diffusion coefficient of the corresponding species. The signal intensities were derived from the integration of the Y25 peak in the corresponding spectrum.

are in accord with our more detailed analysis and suggest that the estimate of 16% folded is the upper limit.

Hydrodynamic Measurements Demonstrate that NTL9 F5A Is Compact in the Absence of Denaturant. The aromatic region of the one-dimensional ^1H NMR spectrum of NTL9 displays a well-resolved resonance from the aromatic ring of Y25. The peak appears at 6.5 ppm in the spectrum of the folded protein and at 6.8 ppm in the F5A spectrum. The hydrodynamic properties of folded wild-type NTL9 and the unfolded mutant can be determined under identical conditions via PFG diffusion measurements using the Tyr resonance. The hydrodynamic radius, R_h, was determined to be 16.1 Å for the wild type. The apparent hydrodynamic radius for F5A in D_2O at pD 5.5 was found to be 20.8 Å (Figure 5). The predicted R_h value is 15.3 Å for a folded 56 residue protein (*19*). F5A was found to populate the unfolded state up to ≥84%; thus, the calculation of the R_h value for the fully populated unfolded state gives a value of 21.7 Å, assuming that a linear extrapolation of R_h is valid. Linear extrapolation of the diffusion coefficients gives an R_h of 21.8 Å. Using the larger estimate of the unfolded state population, 92.5%, R_h of the unfolded state is calculated to be 21.2 Å.

An obvious question is whether the hydrodynamic properties of NTL9 F5A mimic those of the physiologically unfolded state of wild-type NTL9. We suspect that the true unfolded state is more compact than that of the F5A variant since the mutation removes a large hydrophobic group which could disrupt hydrophobic clustering in the unfolded state. It is difficult, and likely impossible, to test this hypothesis directly, but there is indirect evidence that supports it. The hydrodynamic properties of the urea-denatured state of the wild type and F5A can be directly measured. The value of R_h in 8 M urea for the wild type is 23.5 Å, while it is 25.9 Å for F5A (Figure 5). The fact that the unfolded state of F5A is more expanded in urea than that of the wild type suggests, but does not prove, that it may also be more expanded than the true unfolded state in the absence of urea. A similar test was carried out with the F5V variant; the hydrodynamic radius was measured to be 16.2 Å in 100% D_2O and 25.5 Å in 8 M urea (Figure 5). This again suggests that substitution of the phenylalanine with smaller amino acids expands the unfolded state.

NTL9 F5A Contains Residual Secondary Structure. The CD spectrum of F5A indicates the presence of secondary structure. If we assume that the signal at 222 nm is due to α-helical structure, we can estimate the amount of helical structure. This requires an estimate of the CD signal of the fully unfolded form. Here we use the ellipticity measured for F5A in 8 M urea. Using this value to represent the fully unfolded form and using the relationship of Rohl and Baldwin (*31*) to estimate the signal expected for a fully helical system give an estimate of 21% helicity. This corresponds to 12 residues of 56 being helical, making the very crude assumption that a residue is either helical or nonhelical. This estimate of helical content is very crude because it assumes no contribution from the β-sheet structure and assumes a value for an unstructured state. Nonetheless, it provides a basis for comparison to the early peptide fragment studies of NTL9 (*9*). That work showed that a peptide corresponding to the C-terminal α-helix had a significant tendency to fold in isolation, and its estimated helical content was 53%. If similar structure were populated in the intact protein, 13% helical content would be expected. The analysis suggests that more structure is populated in the unfolded state of the intact protein than in the peptide fragment.

CONCLUSIONS

Our work shows that substitution of a single amino acid that disrupts the hydrophobic core of NTL9 is sufficient to populate the unfolded state of this protein under native conditions. Detailed analysis of the thermodynamic properties of the unfolded state created by the Phe to Ala variant was used to quantitatively estimate the extent of unfolded state formation. Comparison of the values of R_h measured for the folded state, NTL9 F5A, and the urea-denatured state of NTL9 shows that the unfolded state populated by NTL9 F5A is more compact than the urea-denatured state. This provides additional evidence that unfolded states contain significant interactions, and the disruption of these interactions under harsh conditions results in alternative conformations. The compact nature of the unfolded state of NTL9 is consistent with our previous observation of the presence of energetically significant interactions in the unfolded state (*17*).

SUPPORTING INFORMATION AVAILABLE

Fluoresence emission spectra of ANS alone, in the presence of F5A, and in the presence of F5A/K12M; far-UV CD scans of F5A/K12M, F5V, and F5V/K12M; plot of absorbance versus radius from an analytical ultracentrifugation experiment with F5A; plot of the CD signal at 222 nm versus denaturant concentration for F5A/K12M. This material is available free of charge via the Internet at http://pubs.acs.org.

REFERENCES

1. Dill, K. A., and Shortle, D. (1991) Denatured states of proteins, *Annu. Rev. Biochem. 60*, 795−825.
2. Tanford, C. (1968) Protein denaturation, *Adv. Protein Chem. 23*, 12−282.
3. Smith, L. J., Fiebig, K. M., Schwalbe, H., and Dobson, C. M. (1996) The concept of a random coil. Residual structure in peptides and denatured proteins, *Folding Des. 1*, R95−R106.
4. Brockwell, D. J., Smith, D. A., and Radford, S. E. (2000) Protein folding mechanisms: New methods and emerging ideas, *Curr. Opin. Struct. Biol. 10*, 16−25.
5. Mok, Y. K., Kay, C. M., Kay, L. E., and Forman-Kay, J. (1999) NOE data demonstrating a compact unfolded state for an SH3 domain under non-denaturing conditions, *J. Mol. Biol. 289*, 619−638.
6. Choy, W. Y., Mulder, F. A. A., Crowhurst, K. A., Muhandiram, D. R., Millett, I. S., Doniach, S., Forman-Kay, J. D., and Kay, L. E. (2002) Distribution of molecular size within an unfolded state ensemble using small-angle X-ray scattering and pulse field gradient NMR techniques, *J. Mol. Biol. 316*, 101−112.
7. Crowhurst, K. A., Tollinger, M., and Forman-Kay, J. D. (2002) Cooperative interactions and a non-native buried Trp in the unfolded state of an SH3 domain, *J. Mol. Biol. 322*, 163−178.
8. Tollinger, M., Crowhurst, K. A., Kay, L. E., and Forman-Kay, J. D. (2003) Site-specific contributions to the pH dependence of protein stability, *Proc. Natl. Acad. Sci. U.S.A. 100*, 4545−4550.
9. Luisi, D. L., Wu, W. J., and Raleigh, D. P. (1999) Conformational analysis of a set of peptides corresponding to the entire primary sequence of the N-terminal domain of the ribosomal protein L9: Evidence for stable native-like secondary structure in the unfolded state, *J. Mol. Biol. 287*, 395−407.
10. Mayor, U., Guydosh, N. R., Johnson, C. M., Grossmann, J. G., Sato, S., Jas, G. S., Freund, S. M., Alonso, D. O., Daggett, V., and Fersht, A. R. (2003) The complete folding pathway of a protein from nanoseconds to microseconds, *Nature 421*, 863−867.
11. Schwalbe, H., Fiebig, K. M., Buck, M., Jones, J. A., Grimshaw, S. B., Spencer, A., Glaser, S. J., Smith, L. J., and Dobson, C. M. (1997) Structural and dynamical properties of a denatured protein. Heteronuclear 3D NMR experiments and theoretical simulations of lysozyme in 8 M urea, *Biochemistry 36*, 8977−8991.
12. Bai, Y., Chung, J., Dyson, H. J., and Wright, P. E. (2001) Structural and dynamic characterization of an unfolded state of poplar apoplastocyanin formed under nondenaturing conditions, *Protein Sci. 10*, 1056−1066.
13. Shortle, D., and Meeker, A. K. (1989) Residual structure in large fragments of staphylococcal nuclease: A heteronuclear NMR study, *Biochemistry 28*, 936−944.
14. Mayor, U., Grossmann, J. G., Foster, N. W., Freund, S. M., and Fersht, A. R. (2003) The denatured state of Engrailed Homeodomain under denaturing and native conditions, *J. Mol. Biol. 333*, 977−991.
15. Kuhlman, B., Boice, J. A., Fairman, R., and Raleigh, D. P. (1998) Structure and stability of the N-terminal domain of the ribosomal protein L9: Evidence for rapid two-state folding, *Biochemistry 37*, 1025−1032.
16. Kuhlman, B., and Raleigh, D. P. (1998) Global analysis of the thermal and chemical denaturation of the N-terminal domain of the ribosomal protein L9 in H_2O and D_2O. Determination of the thermodynamic parameters, $\Delta H°$, $\Delta S°$, and $\Delta C°_p$ and evaluation of solvent isotope effects, *Protein Sci. 7*, 2405−2412.
17. Cho, J. H., Sato, S., and Raleigh, D. P. (2004) Thermodynamics and kinetics of non-native interactions in protein folding: A single point mutant significantly stabilizes the N-terminal domain of L9 by modulating non-native interactions in the denatured state, *J. Mol. Biol. 338*, 827−837.
18. Cho, J. H., and Raleigh, D. P. (2005) Mutational analysis demonstrates that specific electrostatic interactions can play a key role in the denatured state ensemble of proteins, *J. Mol. Biol. 353*, 174−185.
19. Wilkins, D. K., Grimshaw, S. B., Receveur, V., Dobson, C. M., Jones, J. A., and Smith, L. J. (1999) Hydrodynamic radii of native and denatured proteins measured by pulse field gradient NMR techniques, *Biochemistry 38*, 16424−16431.
20. Sato, S. (2002) Folding of ribosomal protein L9 and its isolated N- and C-domains, Ph.D. Thesis, State University of New York, Stony Brook, NY.
21. Laue, T., Shaw, B. D., Ridgeway, T. M., and Pelletier, S. L. (1992) in *Analytical Ultracentrifugation in Biochemistry and Polymer Science* (Harding, S. E., Rowe, A. J., and Horton, J. C., Eds.) The Royal Society of Chemistry, Cambridge, U.K.
22. Wu, D., Chen, A., and Johnson, C. S., Jr. (1995) An improved diffusion-ordered spectroscopy experiment incorporating bipolar-gradient pulses, *J. Magn. Reson., Ser. A 115*, 260−264.
23. Jones, J. A., Wilkins, D. K., Smith, L. J., and Dobson, C. M. (1997) Characterisation of protein unfolding by NMR diffusion measurements, *J. Biomol. NMR 10*, 199−203.
24. Arai, M., and Kuwajima, K. (2000) Role of the molten globule state in protein folding, *Adv. Protein Chem. 53*, 209−282.
25. Mello, C. C., and Barrick, D. (2003) Measuring the stability of partly folded proteins using TMAO, *Protein Sci. 12*, 1522−1529.
26. Horovitz, A., Serrano, L., Avron, B., Bycroft, M., and Fersht, A. R. (1990) Strength and co-operativity of contributions of surface salt bridges to protein stability, *J. Mol. Biol. 216*, 1031−1044.
27. Zdanowski, K., and Dadlez, M. (1999) Stability of the residual structure in unfolded BPTI in different conditions of temperature and solvent composition measured by disulphide kinetics and double mutant cycle analysis, *J. Mol. Biol. 287*, 433−445.
28. Horovitz, A. (1996) Double-mutant cycles: A powerful tool for analyzing protein structure and function, *Folding Des. 1*, R121−R126.
29. Auton, M., and Bolen, D. W. (2005) Predicting the energetics of osmolyte-induced protein folding/unfolding, *Proc. Natl. Acad. Sci. U.S.A. 102*, 15065−15068.
30. Dill, K. A. (1990) Dominant forces in protein folding, *Biochemistry 29*, 7133−7155.
31. Rohl, C. A., and Baldwin, R. L. (1997) Comparison of NH exchange and circular dichroism as techniques for measuring the parameters of the helix−coil transition in peptides, *Biochemistry 36*, 8435−8442.
32. Kraulis, P. J. (1991) MOLSCRIPT: A program to produce both detailed and schematic plots of protein structures, *J. Appl. Crystallogr. 24*, 946−950.

BI060636O